AMERICAN SOCIETY FOR MICROBIOLOGY | mBio®

RESEARCH ARTICLE

Molecular and Structural Analysis of the *Helicobacter pylori cag* Type IV Secretion System Core Complex

Arwen E. Frick-Cheng,[a] Tasia M. Pyburn,[b] Bradley J. Voss,[a] W. Hayes McDonald,[c,d] Melanie D. Ohi,[b,e] Timothy L. Cover[a,f,g]

Department of Pathology, Microbiology and Immunology,[a] Department of Cell and Developmental Biology,[b] Proteomics Laboratory, Mass Spectrometry Research Center,[c] Department of Biochemistry,[d] Center for Structural Biology,[e] and Department of Medicine,[f] Vanderbilt University School of Medicine, Nashville, Tennessee, USA; Veterans Affairs Tennessee Valley Healthcare System, Nashville, Tennessee, USA[g]

ABSTRACT **Bacterial type IV secretion systems (T4SSs) can function to export or import DNA, and can deliver effector proteins into a wide range of target cells. Relatively little is known about the structural organization of T4SSs that secrete effector proteins. In this report, we describe the isolation and analysis of a membrane-spanning core complex from the *Helicobacter pylori cag* T4SS, which has an important role in the pathogenesis of gastric cancer. We show that this complex contains five *H. pylori* proteins, CagM, CagT, Cag3, CagX, and CagY, each of which is required for *cag* T4SS activity. CagX and CagY are orthologous to the VirB9 and VirB10 components of T4SSs in other bacterial species, and the other three Cag proteins are unique to *H. pylori*. Negative stain single-particle electron microscopy revealed complexes 41 nm in diameter, characterized by a 19-nm-diameter central ring linked to an outer ring by spoke-like linkers. Incomplete complexes formed by Δ*cag3* or Δ*cagT* mutants retain the 19-nm-diameter ring but lack an organized outer ring. Immunogold labeling studies confirm that Cag3 is a peripheral component of the complex. The *cag* T4SS core complex has an overall diameter and structural organization that differ considerably from the corresponding features of conjugative T4SSs. These results highlight specialized features of the *H. pylori cag* T4SS that are optimized for function in the human gastric mucosal environment.**

IMPORTANCE **Type IV secretion systems (T4SSs) are versatile macromolecular machines that are present in many bacterial species. In this study, we investigated a T4SS found in the bacterium *Helicobacter pylori*. *H. pylori* is an important cause of stomach cancer, and the *H. pylori* T4SS contributes to cancer pathogenesis by mediating entry of CagA (an effector protein regarded as a "bacterial oncoprotein") into gastric epithelial cells. We isolated and analyzed the membrane-spanning core complex of the *H. pylori* T4SS and showed that it contains unique proteins unrelated to components of T4SSs in other bacterial species. These results constitute the first structural analysis of the core complex from this important secretion system.**

Received 17 November 2015 **Accepted** 24 November 2015 **Published** 12 January 2016

Citation Frick-Cheng AE, Pyburn TM, Voss BJ, McDonald WH, Ohi MD, Cover TL. 2016. Molecular and structural analysis of the *Helicobacter pylori cag* type IV secretion system core complex. mBio 7(1):e02001-15. doi:10.1128/mBio.02001-15.

Editor Martin J. Blaser, New York University

Address correspondence to Melanie D. Ohi, melanie.ohi@vanderbilt.edu, or Timothy L. Cover, timothy.l.cover@vanderbilt.edu.

This article is a direct contribution from a Fellow of the American Academy of Microbiology.

Helicobacter pylori is a Gram-negative bacterium that colonizes the stomach in about half of the world's population (1, 2). Persistent *H. pylori* infection is a risk factor for the development of gastric cancer or peptic ulcer disease (3–5). Adverse disease outcomes associated with *H. pylori* infection occur predominantly in persons infected with strains that produce an effector protein known as CagA (6, 7), which is translocated into host cells through a type IV secretion system (T4SS) (8, 9). The *cagA* gene and genes required for T4SS-dependent secretion of CagA are located within a 40-kb region of the *H. pylori* chromosome known as the *cag* pathogenicity island (*cag* PAI) (10–14). CagA is the only protein known to be secreted by the *H. pylori cag* T4SS. Upon entry into host cells, CagA causes alterations in cell signaling that are linked to gastric carcinogenesis (15–18). *H. pylori*-induced gastric inflammation also contributes to carcinogenesis. *H. pylori* can stimulate gastric epithelial cells to produce and secrete interleukin-8 (IL-8 [a proinflammatory cytokine]) through a T4SS-dependent, CagA-independent process associated with peptidoglycan entry into host cells (9, 19).

T4SSs are a versatile family of secretion systems found in a wide variety of bacterial species (20–22). Three main functional categories of T4SSs are recognized: conjugation systems, effector translocator systems, and DNA release/uptake systems (20). Effector proteins or DNA-protein complexes can be delivered into many types of recipient cells, including mammalian cells, plant cells, fungi, or other bacteria. Examples of DNA-translocating T4SSs include the VirB/VirD4 system found in *Agrobacterium tumefaciens* (which translocates T-DNA into plant cells, causing crown-gall disease) and plasmid conjugation systems (such as the *Escherichia coli* pKM101-encoded Tra system). Effector protein-translocating T4SSs are exemplified by the Dot/Icm systems in *Legionella* and *Coxiella* and the *H. pylori cag* T4SS. Studies of T4SSs from *A. tumefaciens* and plasmid conjugation systems have revealed the existence of a transmembrane channel known as the core complex (23–26). The T4SS core complex encoded by the

E. coli pKM101 conjugative plasmid is composed of three proteins, VirB7/TraN, VirB9/TraO, and VirB10/TraF, which are organized into a ring-like structure, 18.5 nm in diameter, with 14-fold symmetry (24, 25). In comparison to the structural organization of T4SSs that mediate conjugative transfer of DNA, relatively little is known about the structural organization of T4SSs that translocate effector proteins.

Among 18 genes within the *H. pylori cag* pathogenicity island (PAI) that are required for *cag* T4SS-dependent phenotypes (9), several encode proteins that share some sequence relatedness to components of T4SSs in other bacterial species. Notably, the level of sequence conservation is low, and nine of the *cag* PAI genes required for CagA translocation are unique to *H. pylori*, with no obvious homologs in other bacteria (13, 27). This suggests that there are important differences between the *H. pylori cag* T4SS and T4SSs in other bacterial species. Models for the structural organization of the *H. pylori cag* T4SS have been proposed (13, 28–30), but there are numerous limitations and controversial features of the current models, due to a lack of detailed biochemical and structural data. In this report, we describe isolation of the *H. pylori cag* T4SS core complex, biochemical analyses of its composition, and single-particle electron microscopy (EM) analysis of its structure. We show that the *H. pylori cag* T4SS core complex contains proteins that are unrelated to components of T4SSs in other bacterial species and that the architecture of the *H. pylori* core complex differs considerably from that of previously studied T4SS core complexes.

RESULTS

Purification of CagF and copurification of additional Cag proteins. Previous studies have shown that the *H. pylori* cagA effector protein interacts with another *cag* PAI-encoded protein, CagF (31–33). CagF is required for CagA translocation into eukaryotic host cells, and it has been proposed that CagF is a chaperone for CagA (31–33). We hypothesized that the CagF-CagA complex physically interacts with components of the *cag* T4SS machinery and that the CagF-CagA complex could be used as bait for purifying subassemblies of the *cag* T4SS. To test this hypothesis, we generated three *H. pylori* strains that produced hemagglutinin (HA) epitope-tagged forms of CagF; two (HA-CagF and Δ*cagF*/HA-CagF) produced CagF with an N-terminal tag, and one (CagF-HA) produced CagF with a C-terminal tag (see Fig. S1a and b in the supplemental material). The HA-CagF and CagF-HA strains retained the endogenous *cagF* gene (encoding an untagged form of CagF), whereas the Δ*cagF*/HA-CagF strain encoded only the tagged form of CagF. All three strains retained the ability to induce IL-8 secretion in human gastric epithelial (AGS) cells, indicating that the *cag* T4SS is functional in each of these strains (see Fig. S1c).

We immunopurified HA-tagged CagF from lysates of the three *H. pylori* strains using a monoclonal HA antibody, and an untagged wild-type (WT) strain was processed in parallel as a negative control. SDS-PAGE and silver stain analyses showed distinct proteins in preparations derived from the strains producing HA-tagged CagF that were absent in preparations from the untagged WT control strain (see Fig. S1d in the supplemental material). Immunoblotting showed that CagF and CagA were immunopurified from the strains producing HA-tagged CagF, whereas neither of these proteins was immunopurified from the untagged WT control strain (Fig. 1). We then immunoblotted the samples with a panel of antibodies against several components of the *cag* T4SS and found that Cag3, CagT, CagM, CagX, and CagY copurified with CagF and CagA (Fig. 1). Since similar results were obtained with all three strains producing HA-tagged CagF (Fig. 1), we conducted subsequent experiments using strains producing CagF with an N-terminal HA tag (either HA-CagF or Δ*cagF*/HA-CagF).

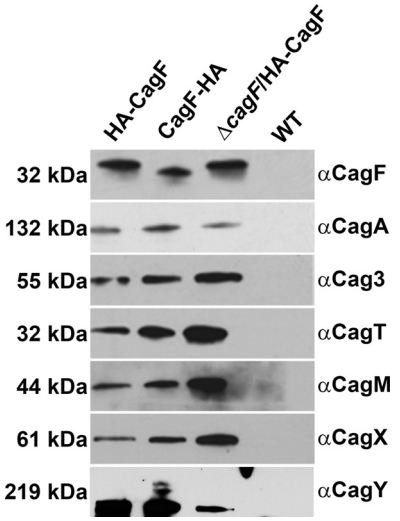

FIG 1 Analysis of proteins that copurify with CagF. Immunoblot analysis of preparations immunopurified from three strains producing HA-tagged CagF using a monoclonal HA antibody and of a control preparation from an untagged WT strain that was processed in parallel. Samples were immunoblotted with the indicated antisera. Results are representative of at least two independent experiments.

Analysis by mass spectrometry indicated that the seven Cag proteins described above (CagF, CagA, Cag3, CagT, CagM, CagX, and CagY) were the most abundant proteins in preparations derived from the HA-CagF-producing strain and that each of these proteins was enriched in preparations from the HA-CagF-producing strain compared to a control preparation from the untagged WT strain (Table 1; see also Table S1 in the supplemental material for complete results). The copurification of several *H. pylori* proteins encoded by genes outside the *cag* PAI and produced at high levels by the bacteria (Table 1) most likely reflects nonspecific interactions (34).

The immunopurifications described above were performed using lysates of *H. pylori* grown in liquid culture. CagA is not actively secreted by the bacteria under such conditions, but *H. pylori* contact with gastric epithelial cells triggers translocation of CagA into the epithelial cells (8, 35). We hypothesized that *H. pylori* contact with gastric epithelial cells leads to activation of the *cag* T4SS, possibly resulting in altered interactions of the CagF-CagA complex with T4SS components. Therefore, we cocultured AGS gastric epithelial cells with HA-CagF-producing *H. pylori* (Δ*cagF*/HA-CagF) and purified HA-CagF from lysates of the coculture. AGS cells cocultured with untagged WT bacteria were processed in parallel as a negative control. Mass spectrometry analysis revealed that preparations isolated from the coculture contained the same seven Cag proteins detected in the earlier experiments (see Table S2 in the supplemental material). Low levels of several other Cag proteins were also detected (see Table S2). Importantly, Cag3, CagT, CagM, CagX, and CagY reproducibly copurified with CagF

TABLE 1 Cag proteins that copurify with HA-CagF

Identified protein	Gene number[b]	Assigned spectral counts[a]	
		HA-CagF	WT
CagA	HP0547	178	0
CagF	HP0543	56	1
CagX	HP0528	40	0
CagM	HP0537	38	0
Cag3	HP0522	44	0
CagT	HP0532	26	0
CagY	HP0527	18	0
No. of Cag spectra		400	1
No. of non-Cag spectra		69	23
Total no. of spectra		469	24

[a] An *H. pylori* strain producing HA-tagged CagF (HA-CagF) was grown in liquid culture, and HA-CagF was immunoaffinity purified using a monoclonal anti-HA antibody. An untagged wild-type strain (WT) was processed in parallel as a control. The protein content of these preparations was analyzed by the use of Multidimensional Protein Identification Technology (MudPIT). The list of *H. pylori* proteins identified was filtered via IDPicker 3.0 using a <5% peptide false-discovery rate (FDR) and a minimum of 2 distinct peptides per protein. The table shows numbers of peptides matched to individual *H. pylori* proteins and lists *cag* PAI-encoded proteins. The complete results are shown in Table S1 in the supplemental material.
[b] Genbank accession number NC_000915.

and CagA in experiments conducted with either bacterial cell-epithelial cell cocultures or bacterial liquid cultures.

Isolation of a Cag protein complex. To investigate whether the proteins copurifying with CagF were constituents of one or more protein complexes, we analyzed immunopurified samples prepared as described above by velocity sedimentation in glycerol density gradients. Immunoblot analysis indicated that Cag3, CagT, CagM, CagX, and CagY cosedimented in the bottom fractions of the gradient (i.e., in the high-molecular-mass fractions) (Fig. 2a). This result provides evidence that Cag3, CagT, CagM, CagX, and CagY are components of a large protein complex. CagA and CagF were detected in the first fraction (taken from the top of the gradient), separately from the other Cag proteins, suggesting that CagF and CagA dissociate from the larger complex during gradient centrifugation. Mass spectrometry analysis of the gradient fractions (Fig. 2b; see also Table S3 in the supplemental material) confirmed that Cag3, CagT, CagM, CagX, and CagY were all distributed in the same gradient fractions (supporting the conclusion that these are components of a protein complex), whereas CagF and CagA were found predominantly in fractions from the top of the gradient (Fig. 2b). Each of the non-Cag proteins present in the sample was detected predominantly in the first fraction (taken from the top of the gradient) instead of the fractions containing Cag3, CagT, CagM, CagX, and CagY (Fig. 2b). Thus, the stringent conditions of the glycerol density gradient allowed purification to homogeneity of a large stable complex of Cag proteins distinct from CagA, CagF, and non-Cag proteins (Fig. 2b; see also Table S3 in the supplemental material).

Cag3, CagT, CagM, CagX, and CagY are all known to be required for T4SS function, including translocation of CagA into host cells (9, 36). Cag3, CagM, and CagT are unique to *H. pylori* and do not exhibit sequence relatedness to constituents of T4SSs in other bacteria, whereas CagX and CagY are orthologs of the VirB9/TraO and VirB10/TraF components of core complexes in DNA-translocating T4SSs (13). Therefore, we reasoned that the Cag protein complex isolated in these experiments corresponds to the *cag* T4SS core complex.

Analysis of complexes formed by mutant strains. We hypothesized that several of the Cag proteins identified in the immunopurification experiments would be required for assembly or stability of the core complex, whereas others would be nonessential for core complex assembly (despite being required for T4SS function). For example, the Cag proteins that have orthologs in T4SSs of multiple bacterial species are likely to be required for core complex formation, whereas proteins unique to *H. pylori* (Cag3, CagT, and CagM) might be dispensable. To test this hypothesis, we analyzed mutant strains in which *cagY*, *cagX*, *cagT*, *cag3*, and *cagM* were individually deleted, and each mutant was engineered to produce HA-CagF, thereby permitting isolation of the core complex. Consistent with the results of previous studies (9), these five mutant strains were unable to induce IL-8 secretion in AGS cells (indicating the absence of a functional *cag* T4SS) (Fig. 3a). We also generated a *cagA* mutant strain that expressed HA-CagF, and, consistent with previous results (9), this strain retained the capacity to induce IL-8 secretion (Fig. 3a). We then sought to isolate Cag protein complexes from the mutant strains by immunopurifying HA-tagged CagF (using the method shown in Fig. 1) and analyzed the resulting preparations by immunoblotting. In experiments performed with Δ*cagX* or Δ*cagY* mutants, we successfully purified CagF and CagA but were unable to copurify core complex com-

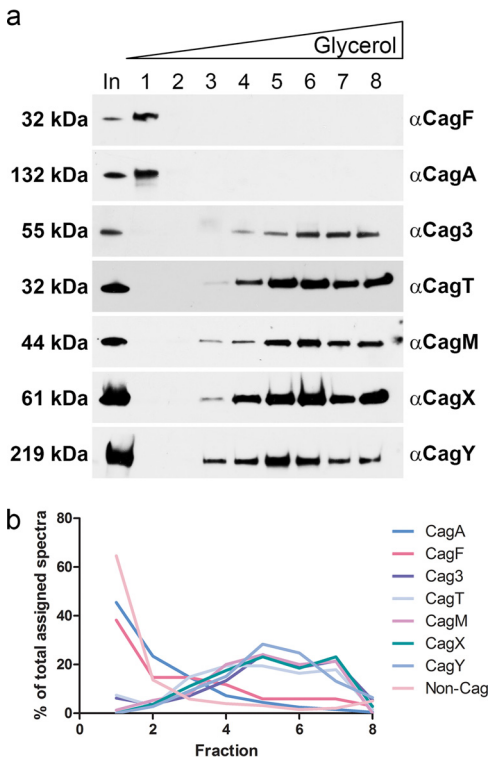

FIG 2 Sedimentation of *H. pylori cag* T4SS core complex in density gradients. (a) Preparations resulting from immunoaffinity purification of HA-CagF were analyzed by velocity sedimentation in glycerol density gradients, and gradient fractions (collected from the top of the gradient) were immunoblotted with the indicated antisera. In, input sample before it was applied to the gradient. Results are representative of two independent experiments. (b) The protein content of gradient fractions was analyzed by 1D mass spectrometry (see Table S3 in the supplemental material for complete results). The distribution of CagF, CagA, Cag3, CagT, CagM, CagX, CagY, and total non-Cag proteins in individual gradient fractions is shown.

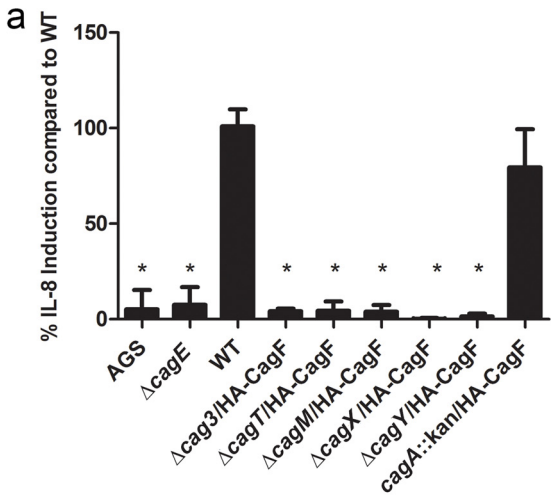

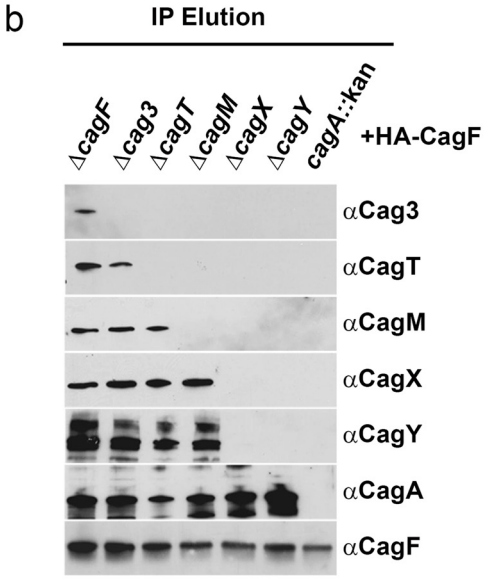

c

	Δcag3	ΔcagT	ΔcagM	ΔcagX	ΔcagY	cagA::kan
Cag3	Absent	Absent	Absent	Absent	Absent	Absent
CagT	Present	Absent	Absent	Absent	Absent	Absent
CagM	Present	Present	Absent	Absent	Absent	Absent
CagX	Present	Present	Present	Absent	Absent	Absent
CagY	Present	Present	Present	Absent	Absent	Absent
CagA	Present	Present	Present	Present	Present	Absent
CagF	Present	Present	Present	Present	Present	Present

FIG 3 Immunopurification of HA-CagF from a panel of *cag* mutant strains. (a) AGS cells were cocultured with the WT strain or the indicated mutants, and IL-8 secretion was quantified by enzyme-linked immunosorbent assay (ELISA). "AGS" indicates cells without added *H. pylori*. Values represent means ± standard deviations (SD), based on analysis of at least six replicate samples. Levels of IL-8 production induced by mutant strains were compared to levels induced by the WT strain (analysis of variance [ANOVA] followed by Dunn's multiple-comparison test). *, $P < 0.001$. (b) HA-CagF was immunoaffinity purified from the strains analyzed in panel A. The affinity-purified samples (immunopurification [IP] elution) were then immunoblotted with the indicated antisera. Strains are designated at the top of the panel, and antisera are designated at the right side of the panel. (c) Summary of results from the experiments presented in panel B, indicating the presence or absence of Cag proteins in the preparations immunopurified from mutant strains. Results are representative of three independent experiments.

ponents (Fig. 3b and c), despite evidence that these proteins were present in lysates from these mutants (see Fig. S2 in the supplemental material). Similarly, in an experiment performed with the *cagA* mutant strain, we successfully purified CagF but were unable to copurify any components of the core complex (Fig. 3b and c). In contrast, we were able to immunopurify multiple Cag proteins as well as CagF and CagA from the Δ*cag3*, Δ*cagT*, *and* Δ*cagM* mutant strains. In experiments performed with the Δ*cag3* strain, all components of the core complex (except Cag3) copurified with CagF and CagA. Preparations immunopurified from the Δ*cagT* strain lacked Cag3 and CagT, and preparations immunopurified from the Δ*cagM* strain lacked Cag3, CagT, and CagM (Fig. 3b and c). These experiments provided evidence that incomplete protein complexes can assemble in the absence of Cag3, CagT, or CagM (Fig. 3b and c).

Ultrastructure analysis of the core complex. We next analyzed the ultrastructure of the *cag* T4SS core complex. *H. pylori* strain HA-CagF (containing an intact *cag* PAI) was grown in liquid culture, complexes were isolated using the CagF-based immunopurification procedure, and the resulting complexes were visualized using negative-stain single-particle EM. EM analysis revealed homogeneous ring-shaped complexes, characterized by well-defined central and outer rings (Fig. 4a). We also used negative-stain single-particle EM to analyze fractions of a glycerol gradient to which the immunopurified sample had been applied, and detected the ring-shaped complexes in the gradient fractions that contained Cag3, CagT, CagM, CagX, and CagY but not in the fractions collected from the top of the gradient (see Fig. S3 in the supplemental material). Since the gradient fractions containing these five Cag proteins were free of other non-Cag proteins (Fig. 2b; see also Table S3 in the supplemental material), this result provides evidence that the complexes visible by EM were composed of Cag proteins.

CagA is not actively secreted during *H. pylori* growth in liquid culture, but coculture of *H. pylori* with gastric epithelial cells is a trigger for translocation of CagA into host cells (8, 35). Therefore, although we did not detect substantial changes in the protein composition of the immunopurified samples in response to epithelial cell contact (see Table S2 in the supplemental material), we hypothesized that the structural organization of the complexes might change when *H. pylori* contacts gastric epithelial cells. To investigate this possibility, we cocultured AGS gastric epithelial cells with HA-CagF-producing *H. pylori*, purified HA-CagF from lysates of the coculture, and then analyzed the immunopurified core complexes by negative-stain EM. The protein complexes isolated from *H. pylori*-AGS cocultures were similar in appearance to the complexes isolated from *H. pylori* liquid cultures, but the complexes isolated from cocultures were present in relatively low abundance and had a less homogeneous appearance (suggestive of degradation) than complexes isolated from liquid cultures (Fig. 4b). Similarly, the complexes in fractions collected from glycerol gradients had suboptimal morphology and exhibited increased clumping compared to complexes in preparations that were not passed through a gradient (see Fig. S3 in the supplemental material). Consequently, all of the subsequent experiments focused on complexes isolated from *H. pylori* grown in liquid culture without use of gradient procedures.

To further characterize the structural features of the complexes, we collected a data set containing a larger number of particles, classified them into 10 class averages using reference-free

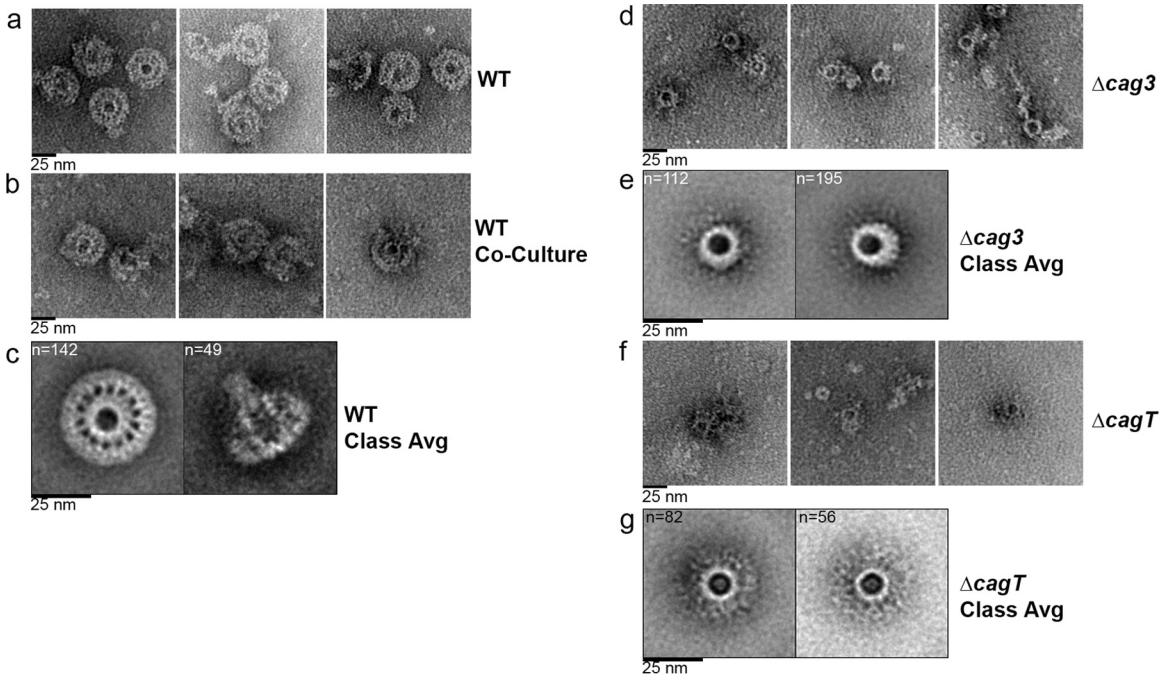

FIG 4 Negative-stain EM analysis of the *H. pylori cag* T4SS core complex. (a) Representative negative-stain images of WT *cag* T4SS complexes purified from a strain with an intact *cag* PAI that was engineered to produce HA-CagF. (b) Representative negative-stain images of WT *cag* T4SS complexes purified from an HA-CagF-producing strain (Δ*cagF*/HA-CagF) cocultured with AGS cells. (c) Class averages (Class Avg) showing an *en face* view and a side view of WT complexes. (d) Representative negative-stain images of *cag* T4SS complexes purified from a Δ*cag3* strain engineered to produce HA-CagF. (e) Class averages of the *cag* T4SS complex purified from a Δ*cag3* strain. (f) Representative negative-stain images of *cag* T4SS complexes purified from a Δ*cagT* strain engineered to produce HA-CagF. (g) Class averages of the *cag* T4SS complex purified from a Δ*cagT* strain. Numbers of particles used for generating each average are shown in upper left corner of panels. All scale bars represent 25 nm.

alignment (see Fig. S4a in the supplemental material), and then selected five of these as references for an additional round of reference-based alignment (see Fig. S4a and b). This analysis revealed well-defined classes, corresponding to *en face* and side views of the T4SS complex (Fig. 4c). The *en face* class shows a well-defined complex, 41 nm in diameter, composed of a central and outer ring connected by short linkers. The central ring is 19 nm in diameter. Fourteen linkers or "spokes" connect the central and outer ring. The side view reveals a stalk-like structure about 40 nm in length, most likely corresponding to the central ring seen in the *en face* views, that extends away from the ring-like portions of the complex.

Ultrastructure analysis of complexes formed by mutant strains. The immunoprecipitation analyses of mutant strains shown in Fig. 3 suggested that incomplete complexes could be formed in the absence of Cag3, CagT, or CagM (Fig. 3b and c). To investigate these incomplete complexes further, we applied the CagF-based immunopurification procedure to these mutant strains and then analyzed the resulting complexes by negative-stain EM. We first imaged preparations derived from the Δ*cagX* mutant (containing CagA and CagF but not any components of the core complex, based on immunoblotting results) (Fig. 3b and c). Consistent with the absence of core complex components detectable by immunoblotting, we did not visualize any ring-like structures in these preparations.

We then imaged complexes isolated from the Δ*cag3* mutant (lacking Cag3 but containing CagX, CagY, CagT, and CagM, based on immunoblot analysis results). The complexes detected in these preparations contained a well-defined ring, but there was a marked reduction in peripheral content and no evidence of a well-organized outer ring (Fig. 4d). To further characterize the structural features of complexes purified from the Δ*cag3* mutant, we collected a data set of particles and generated class averages (see Fig. S4c and d in the supplemental material). These averages revealed *en face* views of a 19-nm-diameter ring (Fig. 4e). Unlike images and classes of wild-type T4SS core complexes, the 2D class averages of complexes isolated from the Δ*cag3* mutant contained no outer ring or connecting spokes (Fig. 4e). The absence of peripheral components in complexes from the Δ*cag3* mutant without any obvious perturbation of the 19-nm-diameter ring provides evidence that Cag3 is localized to the periphery of the complex. To further test this hypothesis, we immunolabeled purified WT core complexes as well as complexes from the Δ*cag3* mutant with primary polyclonal antibodies reactive to Cag3, followed by a secondary antibody conjugated to 5-nm-diameter gold particles. Imaging of the labeled wild-type complexes by negative-stain EM revealed gold particles in the periphery of the complexes, but no gold particles were associated with the central ring (Fig. 5a). Mutant complexes lacking Cag3 were not labeled with gold particles (Fig. 5b), demonstrating the specificity of the immunolabeling. These immunogold EM results corroborated the conclusion that Cag3 is a peripheral component of the *cag* T4SS core complex.

We also imaged complexes isolated from the Δ*cagT* mutant (lacking both Cag3 and CagT). Similarly to complexes isolated from the Δ*cag3* mutant, the complexes isolated from the Δ*cagT*

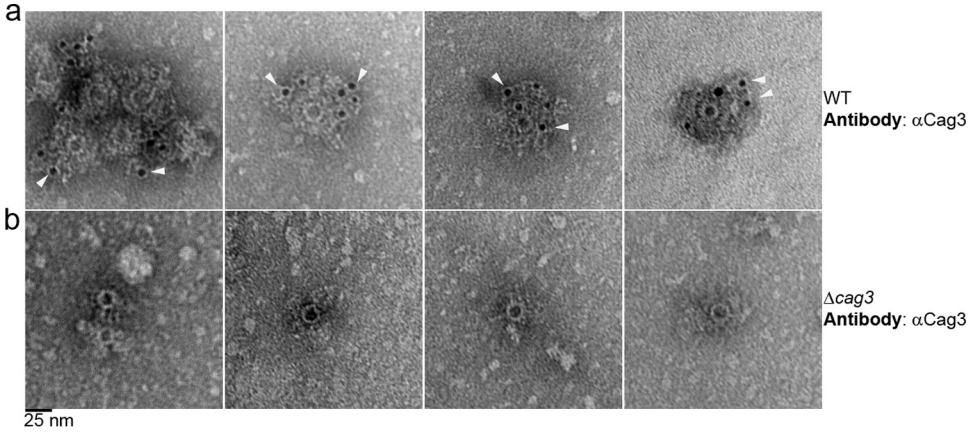

FIG 5 Localization of Cag3 by immunogold labeling and negative-stain EM. Negative-stain EM images of WT core complexes, isolated from a strain with an intact *cag* PAI (a) or a Δ*cag3* mutant (b) and subjected to immunogold labeling with primary anti-Cag3 antiserum followed by 5-nm-diameter-gold-particle-conjugated secondary antibodies, are shown. Arrowheads indicate representative gold particles. Images are representative of results from three independent experiments. Scale bar, 25 nm.

mutant contained a single well-defined ring but no well-organized outer ring (Fig. 4f). The Δ*cagT* mutant complexes were less abundant than the Δ*cag3* mutant complexes. In order to characterize the structural features of complexes purified from the Δ*cagT* mutant, we collected a data set of particles and generated class averages (see Fig. S4e and f in the supplemental material). The *en face* views indicate that the diameter of the ring in complexes from the Δ*cagT* mutant is similar to the diameters of the rings in complexes from the Δ*cag3* mutant and WT strains (Fig. 4g), but the ring in complexes from the Δ*cagT* mutant appears to have a reduced thickness. Unlike images and classes of wild-type T4SS core complexes, the 2D class averages of complexes isolated from the Δ*cagT* mutant contained no outer ring or connecting spokes (Fig. 4g). Immunogold labeling of CagT was attempted using complexes purified from WT and Δ*cagT* strains; however, the results were inconclusive due to the nonspecific binding of the anti-CagT polyclonal antibody under these conditions. We also analyzed preparations derived from the Δ*cagM* mutants (which lack Cag3, CagT, and CagM) but were unable to visualize any ring-shaped complexes in these preparations. The absence of detectable ring-like complexes in preparations from the Δ*cagM* mutant could be due to a reduced stability of these complexes, or, alternatively, ring-shaped complexes may fail to assemble in the absence of CagM. Collectively, the structural differences between mutant and WT complexes, combined with specific antibody labeling, confirm that the ring-like structures seen by negative-stain EM correspond to the T4SS core complex.

DISCUSSION

In this report, we describe the isolation and analysis of a T4SS core complex composed of five different proteins encoded by the *H. pylori cag* pathogenicity island (CagX, CagY, CagM, CagT, and Cag3). Previous studies have detected interactions among several of these Cag proteins (30, 37–39), but the results reported here represent the first successful efforts to isolate and analyze the structure of a complex containing these proteins. Multiple lines of evidence indicate that the complex visualized by EM is composed of Cag proteins. Specifically, glycerol gradient fractions free of contamination from non-Cag proteins contained complexes detectable by EM (see Fig. S3 and Table S3 in the supplemental material), mutant strains lacking Cag3 or CagT formed complexes with a morphology different from that of wild-type complexes (Fig. 4), and Cag3 was detected as a component of the complexes by immunogold staining (Fig. 5).

Each of the 5 protein components of the core complex (CagX, CagY, CagM, CagT, and Cag3) is required for *cag* T4SS-dependent phenotypes, including CagA translocation into host cells and induction of IL-8 secretion by gastric epithelial cells (9). Most of these proteins are also required for production of T4SS-associated pilus structures at the bacterium-host cell interface (36). Previous studies have localized all 5 of these proteins at the outer membrane of *H. pylori* (10, 34). CagX and CagY exhibit low-level sequence relatedness to VirB9 and VirB10 components of T4SSs in other bacterial species, but CagM, CagT, and Cag3 are not closely related to any other bacterial proteins. Sequence analysis of CagT suggests that it may be a lipoprotein, leading to the suggestion that it may be a VirB7 homolog (14). CagA exhibits a high level of sequence variation in comparisons of *H. pylori* strains from different geographic areas, but, in contrast, there is relatively little phylogeographic variation in sequences of the five core complex components (10).

The methodology used in this study for isolating the *H. pylori cag* T4SS core complex relied on immunopurification of CagF, a *cag* PAI-encoded protein that binds the CagA effector protein (31–33). Importantly, velocity sedimentation experiments performed with glycerol gradients indicated that CagF and CagA are not integral components of the core complex. The CagF-based purification strategy conducted with a *cagA* mutant strain failed to yield core complex components, which suggests that CagA directly interacts with the core complex. The interaction of CagA (and possibly CagF) with the core complex is presumably relatively weak, as expected for an interaction of an effector protein with secretion machinery.

The CagF-based immunopurification strategy led to successful isolation of core complexes when applied to bacteria grown in broth culture (a condition under which CagA is not actively secreted), as well as when applied to bacteria cocultured with gastric epithelial cells (a condition that promotes CagA translocation into

a

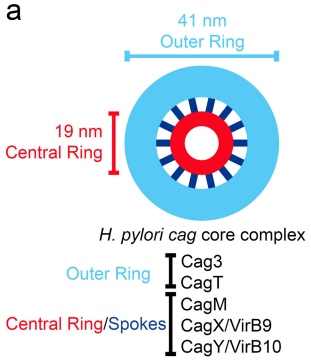

b

Species	Diameter of Core Complex	Components of Core Complex
H. pylori	41 nm	Cag3 CagT CagM CagX/VirB9 CagY/VirB10
E. coli	18.5 nm	TraN/VirB7 TraO/VirB9 TraF/VirB10
L. pneumophila	38 nm	DotG DotD DotH DotF DotC

FIG 6 Schematic model of the *H. pylori cag* T4SS core complex. (a) Prominent features of the complex include an outer ring (light blue) and central ring (red) connected by 14 spokes (dark blue). Analysis of complexes from mutant strains suggests that Cag3 and CagT are localized to the periphery of the intact wild-type complex. (b) Comparison of the diameters and components of T4SS core complexes from *H. pylori*, *E. coli*, and *L. pneumophila*.

the epithelial cells). These results indicate that the core complex is assembled prior to *H. pylori* contact with host cells and CagA translocation. We speculate that CagA is bound to assembled core complexes, ready to be translocated as soon as the bacteria receive the appropriate signal. The molecular mechanisms that regulate CagA secretion (i.e., inhibition of secretion during bacterial growth in broth culture and activation of secretion when *H. pylori* contacts gastric epithelial cells) remain poorly understood.

EM analysis of the isolated core complexes revealed homogeneous ring-shaped structures, 41 nm in diameter, characterized by a central ring connected to an outer ring by thin spoke-like linkers (Fig. 6a). The presence of 14 visible spoke-like linkers in the class averages suggests that the complex may have 14-fold rotational symmetry, but three-dimensional (3D) structural analysis will be required for an accurate assessment of the symmetry. A side view of the complex reveals a long stalk-like domain 40 nm in length that likely corresponds to the central ring seen in the *en face* view. Since all of the core complex components identified in the current study (CagX, CagY, CagT, CagM, and Cag3) have been detected previously on the external surface of *H. pylori* or as components of the outer membrane (30, 34), we propose that the complex is associated primarily with the outer membrane.

Analyses of complexes isolated from a Δ*cag3* mutant strain, along with immunogold labeling experiments, indicate that Cag3 is localized to the periphery of the core complex. Specifically, the complexes formed by the Δ*cag3* mutant strain (containing CagX, CagY, CagM, and CagT, based on immunoblot analysis results) have an intact 19-nm-diameter ring but exhibit a significantly reduced overall diameter compared to wild-type complexes, attributable to loss of the outer ring and spoke-like linkers. We speculate that the substantial loss of peripheral components in complexes from the Δ*cag3* mutant reflects not only the absence of Cag3 but also an alteration in the structure of residual peripheral components so that they are structurally disordered and no longer visible by EM. Complexes isolated from a Δ*cagT* mutant strain (containing CagX, CagY, and CagM, based on immunoblot analysis results) also contained an intact 19-nm-diameter ring and exhibited a loss of visible peripheral components. The complexes from the Δ*cagT* mutant appeared similar to the Δ*cag3* complexes except that the ring appeared to have a reduced thickness. The incomplete complexes derived from Δ*cag3* or Δ*cagT* mutant strains might correspond to intermediate or premature stages in the assembly process that leads to formation of the complete core complex.

Previous studies have analyzed the 3D structure of the T4SS core complex encoded by the *E. coli* pKM101 conjugative plasmid, which is composed of three proteins, VirB7/TraN, VirB9/TraO, and VirB10/TraF (24). The pKM101 T4SS core complex is organized into a ring-like structure, 18.5 nm in diameter, with 14-fold symmetry (24) and is localized primarily to the outer membrane. Core complexes isolated from the *A. tumefaciens* VirB/D4 T4SS are similar in size (about 20 nm in diameter) (40). Therefore, the *H. pylori cag* T4SS core complex (41 nm in diameter) is substantially larger in size than either the pKM101-encoded core complex (25) or *A. tumefaciens* core complex (40) (Fig. 6b). Moreover, the *H. pylori* core complex is composed of five Cag proteins, whereas core complexes from the pKM101 and *A. tumefaciens* T4SSs contain only three (VirB7/TraN, VirB9/TraO, and VirB10/TraF) (24, 25) (Fig. 6b). Despite these differences in size and overall architecture, it is notable that 14 linkers or spokes connecting the central ring to the outer ring could be visualized in the class average of *H. pylori cag* T4SS complexes, which suggests that the *cag* T4SS core complex may have 14-fold rotational symmetry similar to that of the pKM101 core complex. It is also notable that the central ring of the *H. pylori cag* T4SS core complex has a diameter (19 nm) similar to those seen with the T4SS core complexes of *E. coli* and *A. tumefaciens* (24, 40), suggesting that the overall structural organization may be conserved.

Only two components of the *H. pylori cag* T4SS core complex exhibit sequence similarity to components of previously studied T4SS core complexes. Specifically, CagX and CagY exhibit sequence relatedness to VirB9 and VirB10 (Fig. 6b). We propose that CagX and CagY are localized to the central ring of the *cag* T4SS core complex. Consistent with this view, the complexes isolated from Δ*cag3* and Δ*cagT* mutants contained CagX and CagY and had intact rings (with diameters similar to that of the central ring of WT complexes) but lacked the structurally organized outer ring and connecting spokes visualized in WT T4SS complexes.

The exact composition of core complexes in effector protein-translocating T4SSs has not previously been determined for most bacterial species, though the *Legionella* Dot/Icm core complex is reported to contain at least five proteins (DotC, DotD, DotF, DotG, and DotH) (41). Recently published EM images of the *Legionella* Dot/Icm T4SS core complex indicate that it is organized as a circular structure 38 nm in diameter (41). Thus, the size of the *H. pylori* core complex analyzed in the current study is more similar to that of the *Legionella* Dot/Icm core complex than to those of *Agrobacterium* or pKM101 core complexes (Fig. 6b). Another notable similarity between the *H. pylori cag* and *Legionella* Dot/Icm T4SSs is that the core complexes of the two systems have constituents not widely conserved in T4SSs of other bacterial species. Three *H. pylori* core complex constituents (Cag3, CagM, and CagT) seem to be unique species-specific adaptations, and three *Legionella* core complex constituents (DotC, DotF, and DotD) are absent from T4SSs in most other bacterial species. The *H. pylori cag* T4SS translocates CagA across the plasma membrane of gastric epithelial cells, whereas the *Legionella* Dot T4SS translocates several hundred effector proteins across endosomal membranes in eukaryotic cells. The existence of specialized adaptations in *H. py-*

lori and *Legionella* T4SS core complexes is consistent with the considerably different functions of the T4SSs in these two species.

In future studies, it will be important to investigate the molecular mechanisms by which the *H. pylori cag* T4SS mediates CagA translocation into host cells. One possibility is that CagA may pass directly through the central pore visible within the core complex. Analysis of the crystal structure of CagA (amino-terminal residues 1 to 876) indicates that it has dimensions of 8 by 11 by 5.5 nm (17), so either a folded CagA protein or an unfolded CagA protein could conceivably fit through the ~10-nm pore of the core complex. The mechanisms by which CagA enters host cells after translocation across the bacterial envelope remain a topic of inquiry. T4SS-associated pili assembled at the bacterium-host cell interface presumably contribute to the entry of CagA into host cells (42–44), and it has been suggested that binding of CagA to phosphatidylserine or integrins on the surface of host cells also may be important for entry into host cells (18, 45).

In summary, this report provides the first in-depth analysis of the *H. pylori cag* T4SS core complex, which has a key role in the pathogenesis of *H. pylori*-associated gastric diseases, including gastric cancer. The results show that the *cag* T4SS core complex is considerably larger and more complex than core complexes from conjugative T4SSs. Finally, the results highlight the existence of unique species-specific components of the *H. pylori cag* core complex, which presumably represent specialized adaptations optimized for type IV secretion in the human gastric mucosal environment.

MATERIALS AND METHODS

***H. pylori* culture methods and construction of mutants.** For descriptions of the *H. pylori* culture methods and construction of mutants, please refer to Text S1 in the supplemental material.

Isolation of the *H. pylori cag* T4SS core complex. *H. pylori* strains were grown in liquid culture for 16 h (resulting in values of optical density at 600 nm [OD_{600}] of 0.4 to 0.8). Bacterial cells were pelleted at 3,300 × *g* for 15 min at 4°C and resuspended in radioimmunoprecipitation assay (RIPA) buffer (1% NP-40, 0.25% deoxycholate, 10 mM HEPES, and 100 mM NaCl [pH 7.0] supplemented with 1 mM phenylmethylsulfonyl fluoride [PMSF] and protease inhibitors [Complete Mini Protease Inhibitor tablet; Roche]) for initial experiments or in RIPA buffer containing 300 mM NaCl for experiments involving electron microscopy and density gradients. The bacterial suspensions were sonicated on ice and incubated for 1 h at 4°C, and the bacterial lysates were then centrifuged (21,000 × *g*) to pellet insoluble material. Monoclonal anti-HA antibodies were noncovalently linked to protein G Dynabeads (Invitrogen) and incubated with the clarified bacterial lysates at room temperature for 30 min. Beads were washed three times at room temperature with the same buffers used for bacterial lysis, and proteins were selectively eluted with wash buffer containing 200 μg/ml HA peptide (YPYDVPDYA; GenScript). To isolate the core complex from *H. pylori* cocultured with gastric epithelial cells, subconfluent AGS cells were cocultured with *H. pylori* (multiplicity of infection [MOI] of 100) for 4 h. After rinsing with phosphate-buffered saline (PBS) to remove nonadherent bacteria, adherent bacteria and epithelial cells were resuspended in RIPA buffer, and the protocol described above was used.

Glycerol gradients, Western blotting, and mass spectrometric analysis. For details on glycerol gradients, Western blotting, and mass spectrometric analysis, please refer to Text S1 in the supplemental material.

Negative-stain electron microscopy. Samples were prepared for EM as previously described (46). In brief, 5-μl aliquots of samples were absorbed to a glow-discharged 400-mesh copper grid covered with carbon-coated collodion film. Grids were washed in four drops of water and then stained with two drops of uranyl formate (0.75%). Samples were imaged on a Morgagni electron microscope (FEI, Hillsboro, OR) operated at an acceleration voltage of 100 kV and equipped with a 1kx1k charge-coupled-device (CCD) camera (ATM). Images were recorded at a magnification of ×28,000. Images used to generate class averages were collected using a TF20 electron microscope (FEI, Hillsboro, OR) equipped with a field emission gun with an acceleration voltage of 200 kV under low-dose conditions at ×62,000 magnification and a defocus value of ~1.5 μm on a 4kx4k Gatan Ultrascan CCD camera.

Class average generation. Images were converted to mrc (mixed raster content) and binned using a value of 2, resulting in images of 3.5 Å/pixel. For alignment and averaging, 445, 416, and 149 images of wild-type complexes, Δ*cag3* complexes, and Δ*cagT* complexes, respectively, were selected with Boxer and windowed with a 180-pixel side length (63 nm). Image analysis was conducted with Spider (47). The images were rotationally and translationally aligned and subjected to 10 cycles of multireference alignment and K-means classification. For analysis of wild-type complexes, particles were classified into 10 class averages and then 5 representative classes were chosen as references for multireference alignment. For analysis of Δ*cag3* complexes, particles were classified into 20 class averages and then 4 representative projections were chosen as references for another cycle of multireference alignment. For analysis of Δ*cagT* complexes, particles were first classified into 10 class averages and then 3 representative projections were chosen as references for another cycle of multireference alignment.

Immunogold labeling of protein complexes. For details on immunogold labeling of protein complexes, please refer to Text S1 in the supplemental material.

SUPPLEMENTAL MATERIAL

Supplemental material for this article may be found at http://mbio.asm.org/lookup/suppl/doi:10.1128/mBio.02001-15/-/DCSupplemental.

Figure S1, TIF file, 0.4 MB.
Figure S2, TIF file, 0.5 MB.
Figure S3, TIF file, 0.6 MB.
Figure S4, TIF file, 2.2 MB.
Table S1, XLSX file, 0.01 MB.
Table S2, XLSX file, 0.02 MB.
Table S3, XLSX file, 0.01 MB.
Text S1, DOCX file, 0.2 MB.

ACKNOWLEDGMENTS

The work described in this paper was supported by NIH AI039657, CA116087, T32 AI007281, and F31 AI112324 and by the Department of Veterans Affairs (Merit Review grant 2I01BX000627). Proteomics experiments were supported by the Vanderbilt Digestive Diseases Research Center (P30DK058404) and Vanderbilt-Ingram Cancer Center (P30 CA068485).

We thank Charles Sanders for providing helpful advice and the Vanderbilt Center for Structural Biology for support of the microscope facility.

A.E.F.-C., T.L.C., and M.D.O. conceived and designed the experiments. A.E.F.-C. and W.H.M. performed the experiments. A.E.F.-C., T.M.P., B.J.V., T.L.C., and M.D.O. analyzed the data. All authors wrote and approved the manuscript.

FUNDING INFORMATION

HHS | National Institutes of Health (NIH) provided funding to Timothy L. Cover under grant numbers AI039657 and CA116087. HHS | National Institutes of Health (NIH) provided funding to Tasia M. Pyburn under grant number F31 AI112324. HHS | National Institutes of Health (NIH) provided funding to Arwen Frick-Cheng under grant number T32 AI007281. This work was funded by U.S. Department of Veterans Affairs (VA) under grant 2I01BX000627.

REFERENCES

1. **Robin Warren J, Marshall B.** 1983. Unidentified curved bacilli on gastric epithelium in active chronic gastritis. Lancet **321:**1273–1275. http://dx.doi.org/10.1016/S0140-6736(83)92719-8.

2. **Cover TL, Blaser MJ**. 2009. *Helicobacter pylori* in health and disease. Gastroenterology **136:**1863–1873. http://dx.doi.org/10.1053/j.gastro.2009.01.073.
3. **Peek RM, Jr, Blaser MJ**. 2002. *Helicobacter pylori* and gastrointestinal tract adenocarcinomas. Nat Rev Cancer **2:**28–37. http://dx.doi.org/10.1038/nrc703.
4. **Atherton JC**. 2006. The pathogenesis of *Helicobacter pylori*-induced gastroduodenal diseases. Annu Rev Pathol **1:**63–96. http://dx.doi.org/10.1146/annurev.pathol.1.110304.100125.
5. **Suerbaum S, Michetti P**. 2002. *Helicobacter pylori* infection. N Engl J Med **347:**1175–1186. http://dx.doi.org/10.1056/NEJMra020542.
6. **Covacci A, Censini S, Bugnoli M, Petracca R, Burroni D, Macchia G, Massone A, Papini E, Xiang Z, Figura N**. 1993. Molecular characterization of the 128-kDa immunodominant antigen of *Helicobacter pylori* associated with cytotoxicity and duodenal ulcer. Proc Natl Acad Sci U S A **90:**5791–5795. http://dx.doi.org/10.1073/pnas.90.12.5791.
7. **Blaser MJ, Perez-Perez GI, Kleanthous H, Cover TL, Peek RM, Chyou PH, Stemmermann GN, Nomura A**. 1995. Infection with *Helicobacter pylori* strains possessing *cagA* is associated with an increased risk of developing adenocarcinoma of the stomach. Cancer Res **55:**2111–2115.
8. **Odenbreit S, Püls J, Sedlmaier B, Gerland E, Fischer W, Haas R**. 2000. Translocation of *Helicobacter pylori* CagA into gastric epithelial cells by type IV secretion. Science **287:**1497–1500. http://dx.doi.org/10.1126/science.287.5457.1497.
9. **Fischer W, Püls J, Buhrdorf R, Gebert B, Odenbreit S, Haas R**. 2001. Systematic mutagenesis of the *Helicobacter pylori cag* pathogenicity island: essential genes for CagA translocation in host cells and induction of interleukin-8. Mol Microbiol **42:**1337–1348. http://dx.doi.org/10.1046/j.1365-2958.2001.02714.x.
10. **Olbermann P, Josenhans C, Moodley Y, Uhr M, Stamer C, Vauterin M, Suerbaum S, Achtman M, Linz B**. 2010. A global overview of the genetic and functional diversity in the *Helicobacter pylori cag* pathogenicity island. PLoS Genet **6:**e1001069. http://dx.doi.org/10.1371/journal.pgen.1001069.
11. **Tegtmeyer N, Wessler S, Backert S**. 2011. Role of the cag-pathogenicity island encoded type IV secretion system in *Helicobacter pylori* pathogenesis. FEBS J **278:**1190–1202. http://dx.doi.org/10.1111/j.1742-4658.2011.08035.x.
12. **Censini S, Lange C, Xiang Z, Crabtree JE, Ghiara P, Borodovsky M, Rappuoli R, Covacci A**. 1996. cag, a pathogenicity island of *Helicobacter pylori*, encodes type I-specific and disease-associated virulence factors. Proc Natl Acad Sci U S A **93:**14648–14653. http://dx.doi.org/10.1073/pnas.93.25.14648.
13. **Fischer W**. 2011. Assembly and molecular mode of action of the *Helicobacter pylori cag* type IV secretion apparatus. FEBS J **278:**1203–1212. http://dx.doi.org/10.1111/j.1742-4658.2011.08036.x.
14. **Akopyants NS, Clifton SW, Kersulyte D, Crabtree JE, Youree BE, Reece CA, Bukanov NO, Drazek ES, Roe BA, Berg DE**. 1998. Analyses of the cag pathogenicity island of *Helicobacter pylori*. Mol Microbiol **28:**37–53. http://dx.doi.org/10.1046/j.1365-2958.1998.00770.x.
15. **Nešić D, Buti L, Lu X, Stebbins CE**. 2014. Structure of the *Helicobacter pylori* CagA oncoprotein bound to the human tumor suppressor ASPP2. Proc Natl Acad Sci U S A **111:**1562–1567. http://dx.doi.org/10.1073/pnas.1320631111.
16. **Hatakeyama M**. 2014. *Helicobacter pylori* CagA and gastric cancer: a paradigm for hit-and-run carcinogenesis. Cell Host Microbe **15:**306–316. http://dx.doi.org/10.1016/j.chom.2014.02.008.
17. **Hayashi T, Senda M, Morohashi H, Higashi H, Horio M, Kashiba Y, Nagase L, Sasaya D, Shimizu T, Venugopalan N, Kumeta H, Noda N, Inagaki F, Senda T, Hatakeyama M**. 2012. Tertiary structure-function analysis reveals the pathogenic signaling potentiation mechanism of *Helicobacter pylori* oncogenic effector CagA. Cell Host Microbe **12:**20–33. http://dx.doi.org/10.1016/j.chom.2012.05.010.
18. **Kaplan-Türköz B, Jiménez-Soto LF, Dian C, Ertl C, Remaut H, Louche A, Tosi T, Haas R, Terradot L**. 2012. Structural insights into *Helicobacter pylori* oncoprotein CagA interaction with β1 integrin. Proc Natl Acad Sci U S A **109:**14640–14645. http://dx.doi.org/10.1073/pnas.1206098109.
19. **Viala J, Chaput C, Boneca IG, Cardona A, Girardin SE, Moran AP, Athman R, Mémet S, Huerre MR, Coyle AJ, DiStefano PS, Sansonetti PJ, Labigne A, Bertin J, Philpott DJ, Ferrero RL**. 2004. Nod1 responds to peptidoglycan delivered by the *Helicobacter pylori cag* pathogenicity island. Nat Immunol **5:**1166–1174. http://dx.doi.org/10.1038/ni1131.
20. **Alvarez-Martinez CE, Christie PJ**. 2009. Biological diversity of prokaryotic type IV secretion systems. Microbiol Mol Biol Rev **73:**775–808. http://dx.doi.org/10.1128/MMBR.00023-09.
21. **Fronzes R, Christie PJ, Waksman G**. 2009. The structural biology of type IV secretion systems. Nat Rev Microbiol **7:**703–714. http://dx.doi.org/10.1038/nrmicro2218.
22. **Wallden K, Rivera-Calzada A, Waksman G**. 2010. Type IV secretion systems: versatility and diversity in function. Cell Microbiol **12:**1203–1212. http://dx.doi.org/10.1111/j.1462-5822.2010.01499.x.
23. **Christie PJ, Cascales E**. 2005. Structural and dynamic properties of bacterial type IV secretion systems. Mol Membr Biol **22:**51–61. http://dx.doi.org/10.1080/09687860500063316.
24. **Fronzes R, Schäfer E, Wang L, Saibil HR, Orlova EV, Waksman G**. 2009. Structure of a type IV secretion system core complex. Science **323:**266–268. http://dx.doi.org/10.1126/science.1166101.
25. **Chandran V, Fronzes R, Duquerroy S, Cronin N, Navaza J, Waksman G**. 2009. Structure of the outer membrane complex of a type IV secretion system. Nature **462:**1011–1015. http://dx.doi.org/10.1038/nature08588.
26. **Low HH, Gubellini F, Rivera-Calzada A, Braun N, Connery S, Dujeancourt A, Lu F, Redzej A, Fronzes R, Orlova EV, Waksman G**. 2014. Structure of a type IV secretion system. Nature **508:**550–553. http://dx.doi.org/10.1038/nature13081.
27. **Cendron L, Zanotti G**. 2011. Structural and functional aspects of unique type IV secretory components in the *Helicobacter pylori cag*-pathogenicity island. FEBS J **278:**1223–1231. http://dx.doi.org/10.1111/j.1742-4658.2011.08038.x.
28. **Terradot L, Waksman G**. 2011. Architecture of the *Helicobacter pylori cag*-type IV secretion system. FEBS J **278:**1213–1222. http://dx.doi.org/10.1111/j.1742-4658.2011.08037.x.
29. **Bourzac KM, Guillemin K**. 2005. *Helicobacter pylori*-host cell interactions mediated by type IV secretion. Cell Microbiol **7:**911–919. http://dx.doi.org/10.1111/j.1462-5822.2005.00541.x.
30. **Kutter S, Buhrdorf R, Haas J, Schneider-Brachert W, Haas R, Fischer W**. 2008. Protein subassemblies of the *Helicobacter pylori* Cag type IV secretion system revealed by localization and interaction studies. J Bacteriol **190:**2161–2171. http://dx.doi.org/10.1128/JB.01341-07.
31. **Pattis I, Weiss E, Laugks R, Haas R, Fischer W**. 2007. The *Helicobacter pylori* CagF protein is a type IV secretion chaperone-like molecule that binds close to the C-terminal secretion signal of the CagA effector protein. Microbiology **153:**2896–2909. http://dx.doi.org/10.1099/mic.0.2007/007385-0.
32. **Bonsor DA, Weiss E, Iosub-Amir A, Reingewertz TH, Chen TW, Haas R, Friedler A, Fischer W, Sundberg EJ**. 2013. Characterization of the translocation-competent complex between the *Helicobacter pylori* oncogenic protein CagA and the accessory protein CagF. J Biol Chem **288:**32897–32909. http://dx.doi.org/10.1074/jbc.M113.507657.
33. **Couturier MR, Tasca E, Montecucco C, Stein M**. 2006. Interaction with CagF is required for translocation of CagA into the host via the *Helicobacter pylori* type IV secretion system. Infect Immun **74:**273–281. http://dx.doi.org/10.1128/IAI.74.1.273-281.2006.
34. **Voss BJ, Gaddy JA, McDonald WH, Cover TL**. 2014. Analysis of surface-exposed outer membrane proteins in *Helicobacter pylori*. J Bacteriol **196:**2455–2471. http://dx.doi.org/10.1128/JB.01768-14.
35. **Stein M, Rappuoli R, Covacci A**. 2000. Tyrosine phosphorylation of the *Helicobacter pylori* CagA antigen after cag-driven host cell translocation. Proc Natl Acad Sci U S A **97:**1263–1268. http://dx.doi.org/10.1073/pnas.97.3.1263.
36. **Johnson EM, Gaddy JA, Voss BJ, Hennig EE, Cover TL**. 2014. Genes required for assembly of pili associated with the *Helicobacter pylori cag* type IV secretion system. Infect Immun **82:**3457–3470. http://dx.doi.org/10.1128/IAI.01640-14.
37. **Busler VJ, Torres VJ, McClain MS, Tirado O, Friedman DB, Cover TL**. 2006. Protein-protein interactions among *Helicobacter pylori cag* proteins. J Bacteriol **188:**4787–4800. http://dx.doi.org/10.1128/JB.00066-06.
38. **Pinto-Santini DM, Salama NR**. 2009. Cag3 is a novel essential component of the *Helicobacter pylori* Cag type IV secretion system outer membrane subcomplex. J Bacteriol **191:**7343–7352. http://dx.doi.org/10.1128/JB.00946-09.
39. **Jurik A, Hausser E, Kutter S, Pattis I, Prassl S, Weiss E, Fischer W**. 2010. The coupling protein Cagbeta and its interaction partner CagZ are required for type IV secretion of the *Helicobacter pylori* CagA protein. Infect Immun **78:**5244–5251. http://dx.doi.org/10.1128/IAI.00796-10.

40. **Sarkar MK, Husnain SI, Jakubowski SJ, Christie PJ**. 2013. Isolation of bacterial type IV machine subassemblies. Methods Mol Biol **966:**187–204. http://dx.doi.org/10.1007/978-1-62703-245-2_12.
41. **Kubori T, Koike M, Bui XT, Higaki S, Aizawa S-, Nagai H**. 2014. Native structure of a type IV secretion system core complex essential for Legionella pathogenesis. Proc Natl Acad Sci U S A **111:**11804–11809. http://dx.doi.org/10.1073/pnas.1404506111.
42. **Rohde M, Püls J, Buhrdorf R, Fischer W, Haas R**. 2003. A novel sheathed surface organelle of the *Helicobacter pylori cag* type IV secretion system. Mol Microbiol **49:**219–234. http://dx.doi.org/10.1046/j.1365-2958.2003.03549.x.
43. **Shaffer CL, Gaddy JA, Loh JT, Johnson EM, Hill S, Hennig EE, McClain MS, McDonald WH, Cover TL**. 2011. *Helicobacter pylori* exploits a unique repertoire of type IV secretion system components for pilus assembly at the bacteria-host cell interface. PLoS Pathog **7:**e1002237. http://dx.doi.org/10.1371/journal.ppat.1002237.
44. **Kwok T, Zabler D, Urman S, Rohde M, Hartig R, Wessler S, Misselwitz R, Berger J, Sewald N, König W, Backert S**. 2007. Helicobacter exploits integrin for type IV secretion and kinase activation. Nature **449:**862–866. http://dx.doi.org/10.1038/nature06187.
45. **Murata-Kamiya N, Kikuchi K, Hayashi T, Higashi H, Hatakeyama M**. 2010. *Helicobacter pylori* exploits host membrane phosphatidylserine for delivery, localization, and pathophysiological action of the CagA oncoprotein. Cell Host Microbe **7:**399–411. http://dx.doi.org/10.1016/j.chom.2010.04.005.
46. **Ohi M, Li Y, Cheng Y, Walz T**. 2004. Negative staining and image classification—powerful tools in modern electron microscopy. Biol Proced Online **6:**23–34. http://dx.doi.org/10.1251/bpo70.
47. **Shaikh TR, Gao H, Baxter WT, Asturias FJ, Boisset N, Leith A, Frank J**. 2008. Spider image processing for single-particle reconstruction of biological macromolecules from electron micrographs. Nat Protoc **3:**1941–1974. http://dx.doi.org/10.1038/nprot.2008.156.